General Disclaimer

One or more of the Following Statements may affect this Document

- This document has been reproduced from the best copy furnished by the organizational source. It is being released in the interest of making available as much information as possible.

- This document may contain data, which exceeds the sheet parameters. It was furnished in this condition by the organizational source and is the best copy available.

- This document may contain tone-on-tone or color graphs, charts and/or pictures, which have been reproduced in black and white.

- This document is paginated as submitted by the original source.

- Portions of this document are not fully legible due to the historical nature of some of the material. However, it is the best reproduction available from the original submission.

Produced by the NASA Center for Aerospace Information (CASI)

Exchange and relaxation effects in low-energy

radiationless transitions*

Mau Hsiung Chen and Bernd Crasemann

Department of Physics, University of Oregon

Eugene, Oregon 97403

Michio Aoyagi

Ames Research Center, NASA, Moffett Field, California, 94035

Hans Mark

Department of the Air Force, Washington, D. C., 20330

The effect on low-energy atomic inner-shell Coster-Kronig and
super Coster-Kronig transitions that is produced by relaxation and
by exchange between the continuum electron and bound electrons has
been examined and illustrated by specific calculations for transitions
that deexcite the [3p] vacancy state of Zn. Taking exchange and
relaxation into account is found to reduce, but not to eliminate, the
discrepancies between theoretical rates and measurements.
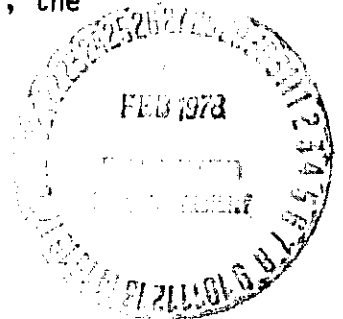
I. INTRODUCTION

In all early Hartree-Fock-Slater (HFS) calculations[1,2] of radiation-less transition rates in atoms with an inner-shell hole, frozen orbitals have been assumed. The wave function of the continuum electron is calculated in the V^{N-1} potential of the initial configuration, as though the continuum electron sees the same potential as the bound electrons in the initial state. In this approximation, the exchange potential used in finding the continuum wave function is the average exchange potential of the bound electrons, and not the exchange potential between bound and continuum electrons.

Calculations that include the frozen-orbital approximation have been reasonably successful in predicting probabilities of energetic Auger transitions.[1,2] For Coster-Kronig and super Coster-Kronig transitions, on the other hand, in which the continuum-electron energy is usually quite low, large discrepancies are found between existing theoretical results and measured rates.[3-7] It is of interest to examine to what extent these perplexing discrepancies can be ascribed to the neglect of exchange and relaxation effects. Exchange has indeed been found to be significant in low-energy electron scattering from atoms[8] and in photoionization near threshold,[9] and its influence on low-energy radiationless transitions has recently been noted by McGuire.[4] In this paper, we report on an investigation of exchange and relaxation effects in low-energy Coster-Kronig and super Coster-Kronig transitions, applied specifically to transitions that deexcite the [3p] vacancy state of atomic Zn.

II. THEORY

In frozen-orbital HFS calculations[2-6] of the Auger transition
probability, the wave function of the continuum electron is calculated
in the same potential as that of the bound electrons. The radial equation
then is

$$\left[- \frac{d^2}{dr^2} + \frac{\ell(\ell+1)}{r^2} - \frac{2Z}{r} + V(r) \right] P_{\varepsilon\ell}(r) = EP_{\varepsilon\ell}(r), \qquad (1)$$

where the potential is

$$V(r) = 2 \sum_{n\ell} q(n\ell) \, \mathcal{Y}_0(n\ell n\ell|r) - 6\left[\frac{3}{8\pi}|\rho(r)| \right]^{1/3}. \qquad (2)$$

The quantities $\mathcal{Y}_k(n\ell n'\ell'|r)$ are defined[10] as

$$\mathcal{Y}_k(n\ell n'\ell'|r) = \int_0^r P_{n\ell}(r) \frac{t^k}{r^{k+1}} P_{n'\ell'}(t)dt + \int_r^\infty P_{n\ell}(t) \frac{r^k}{t^{k+1}} P_{n'\ell'}(t)dt. \qquad (3)$$

Here, $\rho(r)$ is the spherically averaged total electronic charge density.

The Slater exchange potential [the last term in $V(r)$] is the "average"
exchange potential for the bound electrons and does not represent the
exchange interaction between bound and continuum electrons. The Slater
exchange term introduces an attractive potential that pulls the continuum
electron inward. The effect of this term on super Coster-Kronig rates is
discussed in Sec. V.

We now proceed to derive the Hartree-Fock (HF) equation for the
continuum electron which contains the correct exchange interaction between

bound and continuum electrons.

The wave functions of the initial and final states of the atom are assumed to be represented by linear combinations of Slater determinants with normalized spin orbitals. In LS coupling, the wave functions are characterized by the total orbital (L) and total spin (S) quantum numbers. For the specific examples considered here, in which super Coster-Kronig and Coster-Kronig processes fill a 3p-shell vacancy in atomic Zn, the transitions can be described as follows:

$$1s^2 2s^2 2p^6 3s^2 3p^5 3d^{10} 4s^2 \; ^2P \rightarrow 1s^2 2s^2 2p^6 3s^2 3p^6 3d^8 (S_c L_c) \varepsilon \ell' \; ^2P, \quad \ell'=1,3,5$$

and

$$1s^2 2s^2 2p^6 3s^2 3p^5 3d^{10} 4s^2 \; ^2P \rightarrow 1s^2 2s^2 2p^6 3s^2 3p^6 3d^9 4s^1 (S_c' L_c') \varepsilon \ell' \; ^2P, \quad \ell'=1,3.$$

Here, $\varepsilon \ell'$ denotes the energy and orbital angular momentum of the Auger electron in the continuum.

We calculate the initial- and final-state wave functions by the HF approach. We assume that the core of the final-state atom is unaffected by the $\varepsilon \ell'$ continuum electron. For the bound electrons, the HF equations for the radial wave functions can be constructed following the standard procedure.[11,12] The HF equation for the continuum state is obtained following Seaton's method.[13]

The final state is formed by adding an electron to the unperturbed atom with N bound electrons and nuclear charge Z. The antisymmetric (N+1)-electron wave function can be expanded in terms of basis functions which are completely antisymmetric under interchange of the coordinates of a pair of bound electrons:

$$\Psi(\Gamma_j|X) = \sum_{i=1}^{N+1} (-1)^{N+1-i}(N+1)^{-1/2}\psi(\Gamma|X^{-i},\vec{x}_i);$$ (4a)

$$\psi(\Gamma|X^{-i},\vec{x}_i) = \psi(\Gamma|X^{-i},\hat{r}_i\sigma_i)\frac{F_\Gamma(r_i)}{r_i}.$$ (4b)

Here, X^{-i} denotes all the coordinates of the N+1 electrons, except those of the ith electron; $F_\Gamma(r)$ is the radial wave function of the continuum electron, and $\hat{r}_i$, σ_i are the angular and spin coordinates of the ith electron, respectively. The complete set of quantum numbers required to specify the atomic system in the state j is $\Gamma_j = \alpha_j L_j S_j \epsilon_j \ell_j L S M_L M_S$. The system of bound atomic electrons is characterized by $\alpha_j L_j S_j$, and the continuum electron, by $\epsilon_j \ell_j$.

The HF equation for the continuum state can be obtained[13] from

$$\int \psi^*(\Gamma|X^{-(N+1)},\hat{r}_{N+1}\ \sigma_{N+1})[H-E][\psi(\Gamma|X^{-(N+1)},\vec{x}_{N+1})-N\psi(\Gamma|X^{-N}\vec{x}_N)]$$

$$\times\ dX^{-(N+1)}d\hat{r}_{N+1}d\sigma_{N+1} = 0.$$ (5)

Upon integrating over angular coordinates and summing over spin, we find for the radial equation of the continuum electron

$$\left\{\frac{d^2}{dr_{N+1}^2} - \frac{\ell_j(\ell_j+1)}{r_{N+1}^2} + \frac{2Z}{r_{N+1}} + k^2\right\} F_\Gamma(r_{N+1}) - 2V_{\Gamma\Gamma}F_\Gamma(r_{N+1})$$

$$- 2W_{\Gamma\Gamma}(r_{N+1}) - \sum_\ell{}' \delta_{\ell\ell_j}\lambda_{\ell\ell_j}P_{n\ell}(r) = 0,$$ (6)

where $\lambda_{\ell\ell_j}$ is the off-diagonal Lagrange multiplier, and we have

$$V_{\Gamma\Gamma}(r_{N+1}) = \int \psi^*(\Gamma|X^{-(N+1)}\hat{r}_{N+1}\sigma_{N+1}) \sum_{i=1}^{N} \frac{1}{r_{N+1,i}} \; \psi \; (\Gamma|X^{-(N+1)}\hat{r}_{N+1}\sigma_{N+1})$$

$$\times \; dX^{-(N+1)}d\hat{r}_{N+1}d\sigma_{N+1} \tag{6a}$$

and

$$W_{\Gamma\Gamma}(r_{N+1}) = -Nr_{N+1} \int \psi^*(\Gamma|X^{-(N+1)}\hat{r}_{N+1}\sigma_{N+1})[H-E]\psi(\Gamma|X^{-N}\vec{X}_N)dX^{-(N+1)}$$

$$\times \; d\hat{r}_{N+1}d\sigma_{N+1}. \tag{6b}$$

The direct term $V_{\Gamma\Gamma}$ and the exchange term $W_{\Gamma\Gamma}$ were evaluated by the method of Hartree[10] and Racah,[14] and the results were checked against other existing calculations.[15,16]

We shall work out the specific cases of $3p-3d^2\varepsilon\ell'(\ell'=1,3,5)$ and $3p-3d4s\varepsilon\ell'$ $(\ell'=1,3)$ radiationless transitions in atomic Zn. For these transitions, $V_{\Gamma\Gamma}$ and $W_{\Gamma\Gamma}$ can be expressed as follows.

$$V_{\Gamma\Gamma} = \sum_{n\ell} q(n\ell) \mathcal{Y}_0(n\ell n\ell|r) \; + a\mathcal{Y}_2(3d3d|r) + b\mathcal{Y}_4(3d3d|r) \tag{7}$$

and

$$W_{\Gamma\Gamma} = -[2(2\ell'+1)]^{-1}\sum_{ns} q(ns) \mathcal{Y}_{\ell'}(ns\varepsilon\ell'|r)P(ns)$$

$$- \sum_{np} \Big\{ [3\ell'/(2\ell'+1)(2\ell'-1)] \mathcal{Y}_{\ell'-1}(np\varepsilon\ell'|r)P(np)$$

$$+[(3\ell'+1)/(2\ell'+3)(2\ell'+1)] \mathcal{Y}_{\ell'+1}(np\varepsilon\ell'|r)P(np) \Big\}$$

$$-c\mathcal{Y}_{\ell'-2}(3d\varepsilon\ell'|r)P(3d) \; - d\mathcal{Y}_{\ell'}(3d\varepsilon\ell'|r)P(3d)$$

$$-e\mathcal{Y}_{\ell'+2}(3d\varepsilon\ell'|r)P(3d) \; - f\mathcal{Y}_{\ell'}(4s\varepsilon\ell'|r)P(4s). \tag{8}$$

Here, the sum in V_{rr} extends over all occupied shells (i.e., 1s, 2s, 2p, ...) in the final atom, after the Auger transition. The number of electrons in a shell $n\ell$ is denoted by $q(n\ell)$. We have ns = 1s, 2s, 3s, 4s and np = 2p, 3p. The radial wave function of the $n\ell$ bound electron in the final atom is $P(n\ell)$. The coefficients a, b, c, d, e, f are given in Table I.

In deriving Eqs. (6), (7), and (8), it has been assumed that the orbitals are mutually orthogonal. This assumption involves no loss of generality for the continuum wave functions, because there is no open shell in the final atom having the same orbital symmetry as the continuum electron. In Eq. (3), terms with off-diagonal Lagrange multipliers are added in the HF equation for the ϵp continuum electron to insure ortho-gonality.

Using the orthogonality requirement, one can obtain the off-diagonal Lagrange multipliers[17] $\lambda_{2p,\epsilon p}$ and $\lambda_{3p,\epsilon p}$ from the HF equation for the continuum electron [Eq. (3)] and the HF equations for the 2p and 3p bound electrons of the final atom. The expression for $\lambda_{np,\epsilon p}$ is

$$\lambda_{np,\epsilon p} = a'R_1(np3d;3d\epsilon p) + b'R_3(np3d;3d\epsilon p)$$
$$+ c'R_2(np3d;\epsilon p3d) + d'R_1(n;4s;4s\epsilon p), \tag{9}$$

where we have np = 2p or 3p, and

$$R_k(n_1\ell_1 n_2\ell_2;n_3\ell_3 \, n_4 \, _4) = \iint P_{n_1\ell_1}(r_1)P_{n_2\ell_2}(r_2)\frac{r_<^k}{r_>^{k+1}} P_{n_3\ell_3}(r_1)P_{n_4\ell_4}(r_2)dr_1 dr_2$$

is the generalized Slater integral. The coefficients a', b', c', and d' are listed in Table II.

III. THE RADIATIONLESS TRANSITION PROBABILITY

From Wentzel's ansatz,[18] the radiationless transition probability is given by the familiar formula of perturbation theory,

$$W_{fi} = \hbar^{-2} \left| \left\langle \Psi_f | H-E | \Psi_i \right\rangle \right|^2, \tag{10}$$

where the continuum wave function has been normalized to represent one electron ejected per unit time.[19,20] To take into account the effect of relaxation, we calculate the initial and final bound states separately in accordance with their respective hole configurations. The lack of orthogonality between initial and final electron orbitals with the same orbital symmetry causes the expression for the Auger transition probability to contain more terms than in the usual frozen-orbital theory.[21,22] For the $3p$-$3d^2\epsilon\ell$ and $3p$-$3d4s\epsilon\ell$ transitions in atomic Zn, however, there are no contributions from the one-electron operator because of the orthogonality of the angular parts of the wave functions.

The radiationless transition rates for Zn $3p$-shell super Coster-Kronig ($3p$-$3d^2\epsilon\ell$) and Coster-Kronig ($3p$-$3d4s\epsilon\ell$) transitions, including the effect of relaxation, are given by the following expressions.

$$W_{fi}(3p\to 3d^2) = \hbar^{-2} \Big| K_1 \Big\langle 3p'\epsilon\ell \Big| \frac{1}{r_{12}} \Big| 3d^2 \Big\rangle - \Big[\Big\langle 2p'\epsilon\ell \Big| \frac{1}{r_{12}} \Big| 3d^2 \Big\rangle \Big\langle 3p' \Big| 2p \Big\rangle$$

$$+ \Big\langle 3p'^2 \Big| \frac{1}{r_{12}} \Big| 3d^2 \Big\rangle \Big\langle \epsilon\ell \Big| 3p \Big\rangle \delta_{\ell 1} + \Big\langle 2p'3p' \Big| \frac{1}{r_{12}} \Big| 3d^2 \Big\rangle \Big\langle \epsilon\ell \Big| 2p \Big\rangle \delta_{\ell 1} \Big]$$

$$\times (\text{quantity of order one}) + \ldots \Big|^2, \tag{11}$$

with

$$K_1 = \langle 1s'|1s \rangle^2 \langle 2s'|2s \rangle^2 \langle 2p'|2p \rangle^6 \langle 3s'|3s \rangle^2 \langle 3p'|3p \rangle^5 \langle 3d'|3d \rangle^8 \langle 4s'|4s \rangle^2$$

+ smaller terms containing two or more exchange overlap integrals.

$$W_{fi}(3p \rightarrow 3d4s) = \hbar^{-2} \left| K_2 \langle 3p'\varepsilon\ell \left| \frac{1}{r_{12}} \right| 3d4s \rangle - \left[\langle 2p'\varepsilon\ell \left| \frac{1}{r_{12}} \right| 3d4s \rangle \right. \right.$$
$$\times \langle 3p'|2p \rangle + \langle 3p'^2 \left| \frac{1}{r_{12}} \right| 3d4s \rangle \langle \varepsilon\ell|3p \rangle \delta_{\ell 1}$$
$$\left. \left. + \langle 3p'\varepsilon\ell \left| \frac{1}{r_{12}} \right| 3d3s \rangle \langle 3s'|4s \rangle \right] \times \text{(quantity of order one)} + \ldots \right|^2, \quad (12)$$

with

$$K_2 = \langle 1s'|1s \rangle^2 \langle 2s'|2s \rangle^2 \langle 2p'|2p \rangle^6 \langle 3s'|3s \rangle^2 \langle 3p'|3p \rangle^5 \langle 3d'|3d \rangle^9 \langle 4s'|4s \rangle$$

+ smaller terms containing two or more exchange overlap integrals.

In the present calculations we neglect terms with one or more exchange overlap integrals, such as $\langle 3p'|2p \rangle$, $\langle \varepsilon\ell|3p \rangle$. Then the radiationless transition rates become

$$W_{fi}(3p \rightarrow 3d^2) = \hbar^{-2} K_1^2 \left| \langle 3p'\varepsilon\ell \left| \frac{1}{r_{12}} \right| 3d^2 \rangle \right|^2 \quad (13)$$

and

$$W_{fi}(3p \rightarrow 3d4s) = \hbar^{-2} K_2^2 \left| \langle 3p'\varepsilon\ell \left| \frac{1}{r_{12}} \right| 3d4s \rangle \right|^2 . \quad (14)$$

The two-electron Auger matrix elements, expressed in terms of generalized Slater integrals, were calculated using Racah algebra.[14] The relevant expressions[21,22] are given in Table III.

IV. NUMERICAL METHOD

The initial and final bound-state wave functions were calculated with Froese-Fischer's Hartree-Fock program.[12] An iterative procedure was

used to solve the HF equations for the continuum state, the first solution being obtained by ignoring the exchange terms. The iterations were continued until the maximum relative error in the wave functions became less than 10^{-4}. In general, the solutions converged to this extent within 6 iterations for εf and εh states, and within 20 iterations for εp states. This convergence criterion was found to lead to consistency to four significant figures in the Auger radial matrix element.

The 3p-shell super Coster-Kronig and Coster-Kronig transition energies were calculated as well with the Froese-Fischer HF program,[12] including relaxation. The calculated energies are compared with experimental results in Table IV.

V. RESULTS AND DISCUSSION

A. Frozen-orbital approximation

In order to study the sensitivity of the super Coster-Kronig transition probability on wave functions and energy,[4,23] we have calculated these transition probabilities on the basis of several frozen-orbital models. To distinguish various models, we shall use N to denote the number of bound electrons in a neutral atom (i.e., N=Z). Results for the Zn 3p-$3d^2(^3F;^1G)\varepsilon f$ transitions are shown in Fig. 1. To calculate the rates labeled "HF V^{N-1}", initial-configuration HF bound-state wave functions were used for both initial and final bound states; the continuum wave function was calculated in the V^{N-1} potential of the (singly ionized) initial

configuration, without exchange. The "HF V^N" rates were calculated by a similar procedure, the only difference being that the HF bound-state wave functions of the neutral atom were used. The "HFS V^{N-1}" rates were calculated with Herman-Skillman[24] HFS wave functions for the initial hole state, employed for both the initial and final bound states; the continuum wave function here is the solution of Eq. (1) with $V(r)$ [Eq. (2)] taken to be the average potential for the initial state.

It is clear from Fig. 1 that the Zn $3p$-$3d^2(^3F;{}^1G)\epsilon f$ transitions are quite sensitive to the transition energy and to the details of the wave functions. The frozen HFS V^{N-1} rates, for example, are much larger than those derived for the HF V^{N-1} model. Most of this difference can be attributed to the fact that $V(r)$ [Eq. (1)] in the HFS V^{N-1} model contains the wrong exchange term.

B. Exchange and relaxation effects on 3p-shell Coster-Kronig and super Coster-Kronig transitions in Zn

To investigate how exchange affects the transition rates, calculations were performed with different continuum wave functions. The continuum wave functions were found by solving Eq. (6) (1) neglecting the exchange term W_{rr}, and (2) including the exchange term W_{rr}. In Figs. 2 and 3 we have plotted the continuum wave functions for $3p$-$3d^2(^1G)\epsilon f$ and $3p$-$3d^2(^1S)\epsilon p$ transitions, respectively; the transition energy was taken to be 42 eV in both cases, equal to the average observed energy.[25] Also shown in Figs. 2 and 3 is the HF 3d wave function of the final atom.

It can be noted in Fig. 2 that there is very little cancellation in the overlap between 3d and εf wave functions. The $3p-3d^2(^3F)\varepsilon f$ and $3p-3d^2(^1G)\varepsilon f$ rates are therefore large and very sensitive to energy and wave functions. By contrast, Fig. 3 shows that in $3p-3d^2(^1S;^3P;^1D)\varepsilon p$ transitions strong cancellation occurs in the overlap between 3d and εp wave functions. These transition rates are therefore small. The inclusion of exchange is seen to pull the continuum wave function in toward the origin, causing the $3d^2\varepsilon f$ transition probabilities to be increased by ~6% (Fig. 2), while the $3d^2(^1S)\varepsilon p$ rate is reduced by ~7% (Fig. 3). The effect of exchange becomes less pronounced as the Auger energy increases.

Using HF instead of HFS bound-state wave functions in the HF continuum equation and in Auger transition probability calculations reduces the transition rates by only ~3% for $\varepsilon = 42$ eV (Fig. 4).

Relaxation is found to affect the transition rates substantially. Relaxation is taken into account by discarding the frozen-orbital approximation and using HF bound-state wave functions corresponding to the appropriate (different) initial and final states in the calculations. The exchange overlap integrals, such as $\langle 2p'|3p\rangle$, $\langle \varepsilon p|3p\rangle$, in Eqs. (11) and (12) are all found to be $\leq 10^{-3}$, so that terms involving these integrals could justifiably be neglected. For the overlap correction factors we find $K_1=0.9239$ and $K_2=0.9895$. In Fig. 4, the $3p-3d^2(^1G)\varepsilon f$ transition probabilities are shown, as calculated with continuum wave functions in the V^{N-2} potential and with different bound-state wave functions. Relaxation is seen to reduce these transition rates by ~20%.

Also included in Fig. 4 are results (labeled "HFS V^{N-2}") that were obtained with HFS initial-configuration bound-state wave functions and with a continuum wave function that is the solution of Eq. (1) with $V(r)$ [Eq. (2)] being the average potential of the final two-hole configuration. Once again, these HFS results are much larger than the rates calculated by other methods, due to the error in the exchange term in $V(r)$ of Eq. (2).

C. Zn $M_{2,3}$-level width

The 3p-level widths of Zn, calculated with different wave functions, are listed in Table V. Average experimental Auger energies of Zn vapor[25] were used in the calculations. The experimental $M_{2,3}$ level width[25] of atomic Zn is listed for comparison. The agreement between the HF V^{N-1} frozen-orbital result with experiment is probably accidental. Results from the relaxed HF model, which can be considered more realistic, agree better with experiment than HFS results but still are 50% too large.

Transition rates to various final states, calculated with the relaxed HF model, are indicated in Table VI.

VI. CONCLUSION

In HFS calculations of radiationless transition rates, the assumption that the continuum electron sees the same potential as the bound electrons can cause a large error in low-energy Coster-Kronig and super Coster-Kronig cases. The HF approach including relaxation removes some but not all of the discrepancy with experiment.

The effect of configuration interaction among discrete states on
3p-shell Coster-Kronig and super Coster-Kronig transitions of Zn
has been found to be small.[4] The importance of the final-state channel
interactions has recently been pointed out by Howat et al.[26] Calculations
to include the channel interactions are in progress.

[1] W. Bambynek, B. Crasemann, R. W. Fink, H.-U. Freund, H. Mark, C. D. Swift, R. E. Price, and P. V. Rao, Rev. Mod. Phys. $\underline{44}$, 716 (1972).

[2] E. J. McGuire, in Atomic Inner-Shell Processes, ed. by B. Crasemann (Academic, New York, 1975), Vol. I, p. 293.

[3] E. J. McGuire, Phys. Rev. A $\underline{11}$, 1880 (1975).

[4] E. J. McGuire, Phys. Rev. A $\underline{16}$, 2365 (1977).

[5] M. O. Krause, F. Wuilleumier, and C. W. Nestor, Jr., Phys. Rev. A $\underline{6}$, 871 (1972).

[6] M. H. Chen, B. Crasemann, M. Aoyagi, and H. Mark, Phys. Rev. A $\underline{15}$, 2312 (1977).

[7] S. Svensson, N. Martensson, E. Basilier, P. A. Malmqvist, U. Gelius, and K. Siegbahn, Physica Scripta $\underline{14}$, 141 (1976).

[8] D. W. Walker, J. Phys. B $\underline{2}$, 356 (1969).

[9] D. J. Kennedy and S. T. Manson, Phys. Rev. A $\underline{5}$, 227 (1972).

[10] D. R. Hartree, The Calculation of Atomic Structures (Wiley, New York, 1957), p. 40.

[11] J. C. Slater, Quantum Theory of Atomic Structure (McGraw-Hill, New York, 1960), Vol. II.

[12] C. Froese-Fischer, Comp. Phys. Commun. $\underline{4}$, 107 (1972); At. Data $\underline{4}$, 301 (1972).

[13]M. J. Seaton, Phil. Trans. Roy. Soc. A245, 469 (1953).

[14]G. Racah, Phys. Rev. 63, 367 (1943).

[15]K. Smith, R. J. W. Henry, and P. G. Burke, Phys. Rev. 147, 21 (1966).

[16]O. Bely, J. Jully, and H. Van Regemorter, Ann. Phys. (Paris) 8, 303 (1963).

[17]A. Dalgarno, R. J. W. Henry, and A. L. Stewart, Planet, Space Sci. 12, 235 (1964).

[18]G. Wentzel, Z. Physik 43, 524 (1927).

[19]J. R. Oppenheimer, Z. Physik 55, 725 (1929).

[20]J. A. Gaunt, Phil. Trans. Roy. Soc. (London) A229, 163 (1930).

[21]R. A. Rubenstein and J. N. Snyder, Phys. Rev. 97, 1653 (1955); R. A. Rubenstein, thesis, University of Illinois, 1955 (unpublished).

[22]V. O. Kostroun, M. H. Chen, and B. Crasemann, Phys. Rev. A 3, 533 (1971).

[23]L. I Yin, I. Adler, T. Tsang, M. H. Chen, D. A. Ringers, and B. Crasemann, Phys. Rev. A 9, 1070 (1974).

[24]F. Herman and S. Skillman, Atomic Structure Calculations (Prentice-Hall, Englewood Cliffs, N.J., 1963).

[25]D. Hausamann, B. Breuckmann, and W. Mehlhorn, in Abstracts of Papers, X International Conference on the Physics of Electronic and Atomic Collisions (Commissariat à l'Energie Atomique, Paris, 1977), Vol. I, p. 208.

[26]G. Howat, T. Åberg, and O. Goscinski, Helsinki University of Technology Laboratory of Physics Research Report No. 14/1977 (unpublished).

TABLE I. Coefficients a, ..., f in Eqs. (7) and (8).

Final hole state Configuration	Term	ℓ'	a	b	c	d	e	f
$3d^2$	^1S	p	0	0	0	8/15	12/35	0
$3d^2$	^3P	p	-1/5	0	0	-7/30	6/35	0
$3d^2$	^1D	p	3/35	0	0	13/30	102/245	0
$3d^2$	^1D	f	24/245	-8/147	2/5	27/451	50/231	0
$3d^2$	^3F	f	-3/35	1/21	-6/35	2/105	50/231	0
$3d^2$	^1G	f	-55/147	-13/147	-12/35	46/245	50/231	0
$3d^2$	^1G	h	-8/21	-2/21	-47/380	50/429	21/143	0
$3d4s$	^1D	p	-1/5	0	0	1/3	3/7	0
$3d4s$	^3D	p	-1/5	0	0	-1/3	3/7	-1/3

TABLE II. Coefficients a', ..., d' in Eq. (9).

| Final hole state | | a' | b' | c' | d' |
Configuration	Term				
$3d^2$	^1S	0	0	0	0
	^3P	-23/15	-12/35	2/5	0
	^1D	-1/5	36/245	-6/35	0
3d4s	^1D	-8/15	3/35	2/5	0
	^3D	-28/15	3/35	2/5	-2/3

TABLE III. The $3p$-$3d^2\epsilon\ell'$ and $3p$-$3d4s\epsilon\ell'$ radiationless transition probabilities, in LS coupling, in terms of radial integrals.

Final hole state Configuration	Term	ℓ'	Transition probability
$3d^2$	^1S	1	$\frac{1}{5}\left|\frac{2}{3} R_1(3p\epsilon p3d3d) + \frac{3}{7} R_3(3p\epsilon p3d3d)\right|^2$
	^3P		$\frac{27}{5}\left|-\frac{1}{3} R_1(3p\epsilon p3d3d) + \frac{1}{7} R_3(3p\epsilon p3d3d)\right|^2$
	^1D		$\frac{1}{35}\left|\frac{7}{3} R_1(3p\epsilon p3d3d) + \frac{3}{7} R_3(3p\epsilon p3d3d)\right|^2$
$3d^2$	^1D	3	$\frac{6}{35}\left|\frac{1}{3} R_1(3p\epsilon f3d3d) + \frac{4}{7} R_3(3p\epsilon f3d3d)\right|^2$
	^3F		$\frac{18}{5}\left|-\frac{1}{3} R_1(3p\epsilon f3d3d) + \frac{1}{7} R_3(3p\epsilon f3d3d)\right|^2$
	^1G		$\frac{2}{35}\left|3 R_1(3p\epsilon f3d3d) + \frac{1}{7} R_3(3p\epsilon f3d3d)\right|^2$
$3d^2$	^1G	5	$\frac{50}{343}\left|R_3(3p\epsilon h3d3d)\right|^2$
$3d4s$	^1D	1	$\frac{1}{9}\left|R_1(3p\epsilon p3d4s) + R_1(3p\epsilon p4s3d)\right|^2$
	^3D		$\frac{1}{3}\left|R_1(3p\epsilon p3d4s) - R_1(3p\epsilon p4s3d)\right|^2$
$3d4s$	^1D	3	$\frac{3}{2}\left|\frac{1}{7} R_3(3p\epsilon f3d4s) + \frac{1}{3} R_1(3p\epsilon f4s3d)\right|^2$
	^3D		$\frac{9}{2}\left|-\frac{1}{7} R_3(3p\epsilon f3d4s) + \frac{1}{3} R_1(3p\epsilon f4s3d)\right|^2$

TABLE IV. The 3p-shell super Coster-Kronig and Coster-Kronig
transition energies of atomic Zn.

| Final state | | Energy (eV) | |
Configuration	Term	Theory	Experiment[a]
$3d^8$	^1S	40.26	
	^3P	46.97	
	^1D	47.49	42.2
	^3F	50.02	
	^1G	46.07	
$3d^94s$	^1D	63.62	59.0
	^3D	64.14	

[a]Measurements on Zn vapor, Ref. 25.

TABLE V.   Zn $M_{2,3}$ level width

Method	Width (eV)
Theory: HFS V^{N-1}	3.25
Theory: HFS V^{N-2}	4.49
Theory: HF V^{N-1}	1.83
Theory: HF V^{N}	1.20
Theory: Relaxed HF	2.93
Experiment[a]	2.1±0.2

[a]Ref. 25.

TABLE VI. Theoretical Zn 3p-shell super Coster-Kronig and Coster-Kronig transition probabilities according to the relaxed HF model.

Transition	Final term	Transition rate (milli atomic units)
3p-3d3dϵp	^{1}S	0.838
	^{3}P	0.575
	^{1}D	0.740
3p-3d3dϵf	^{1}D	8.389
	^{3}F	26.637
	^{1}G	61.370
3p-3d3dϵh	^{1}G	0.021
3p-3d4sϵp	^{1}D	4.690
	^{3}D	3.651
3p-3d4sϵf	^{1}D	0.606
	^{3}D	0.048

Figure Captions

FIG. 1.   Probabilities of the $3p-3d^2(^3F;^1G)\varepsilon f$ transitions in atomic Zn, according to frozen-orbital calculations with various wave functions and potentials: Hartree-Fock in the singly ionized (V^{N-1}) and neutral-atom (V^N) potential, and Hartree-Fock-Slater in the V^{N-1} potential.   To illustrate energy dependence of these rates, the transition energy is treated as a variable.   The measured average transition energy is 42 eV (Ref. 25).

FIG. 2.   The Hartree-Fock bound-state 3d radial wave function of atomic Zn and the εf HF continuum wave function, calculated in the potential of the final atomic state, with and without the exchange term $W_{\Gamma\Gamma}$ in Eq. (6).

FIG. 3.   The HF 3d bound-state radial wave function of Zn and the εp HF continuum wave function, calculated with and without the exchange term $W_{\Gamma\Gamma}$ in Eq. (6).

FIG. 4.   Theoretical $3p-3d^2(^1G)\varepsilon f$ radiationless transition probabilities, as a function of Auger energy, calculated according to various models.   Relaxed Hartree-Fock, frozen Hartree-Fock, and frozen Hartree-Fock-Slater bound-state wave functions are used, all three with a Hartree-Fock continuum wave function in the V^{N-2} potential of the doubly ionized final-state atom, with and without exchange between continuum and bound electrons (Eq. 6).   Only for the top curve (diamonds), the continuum electron is described by a Hartree-Fock-Slater wave function [Eqs. (1) and (2)].
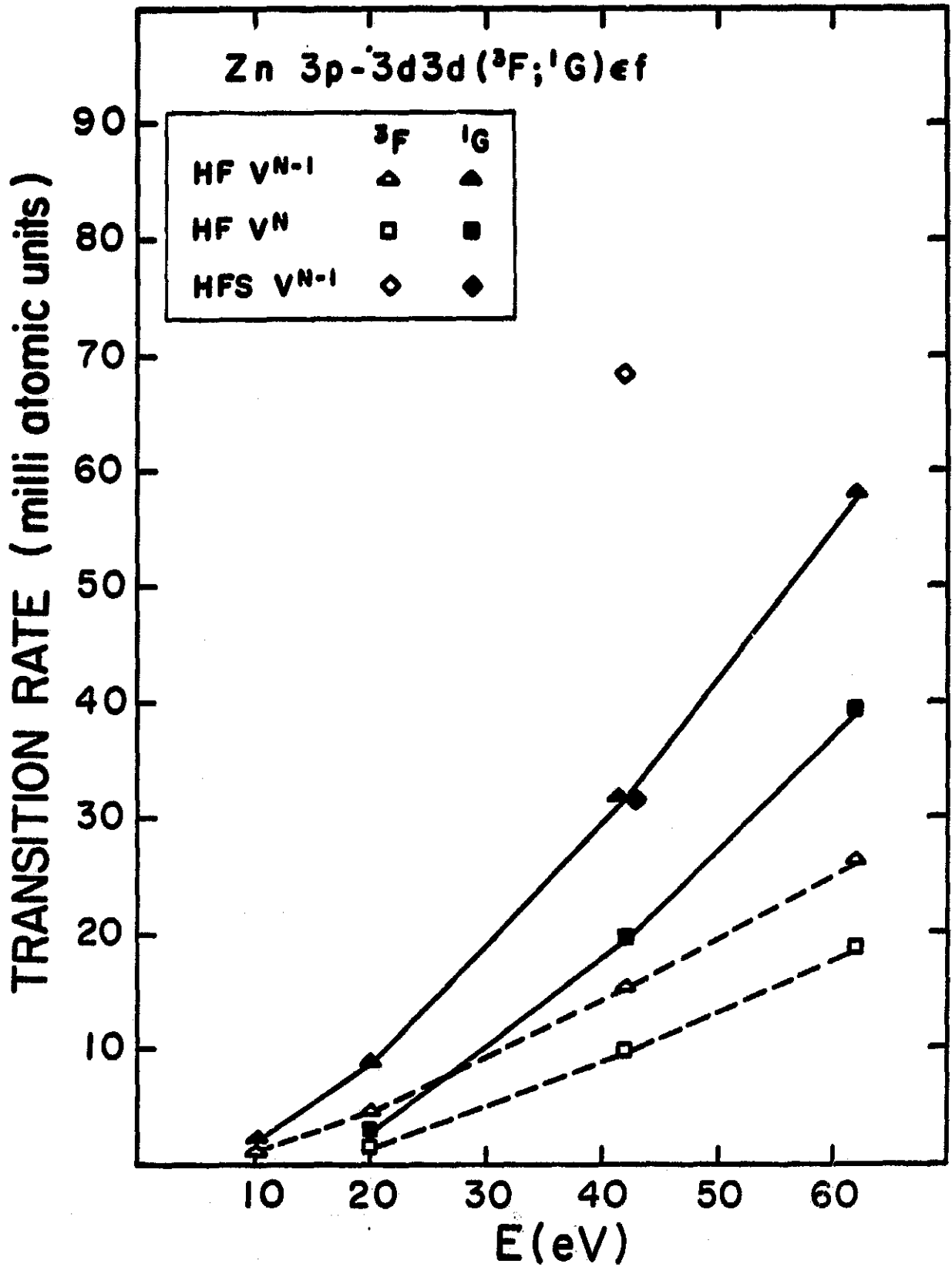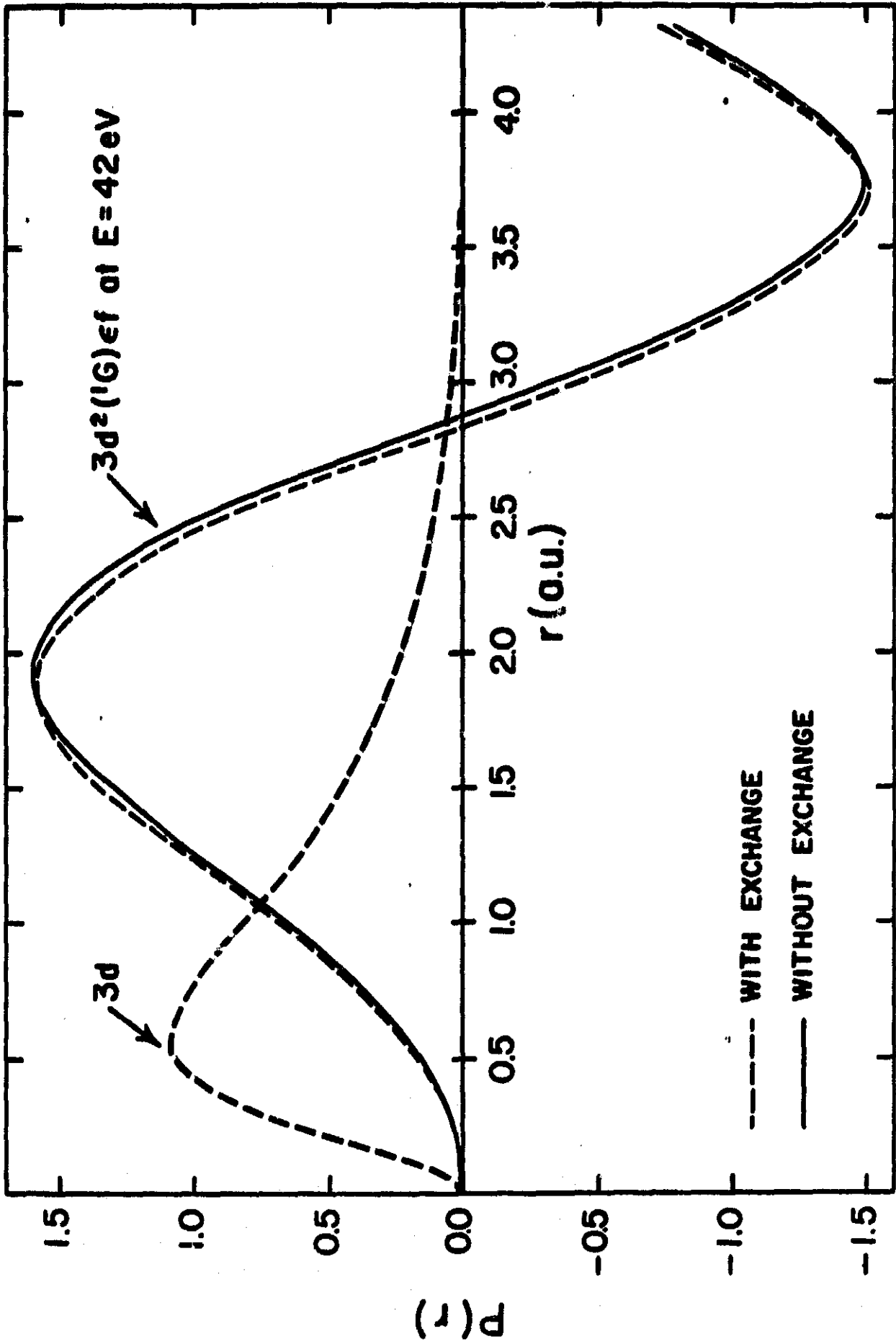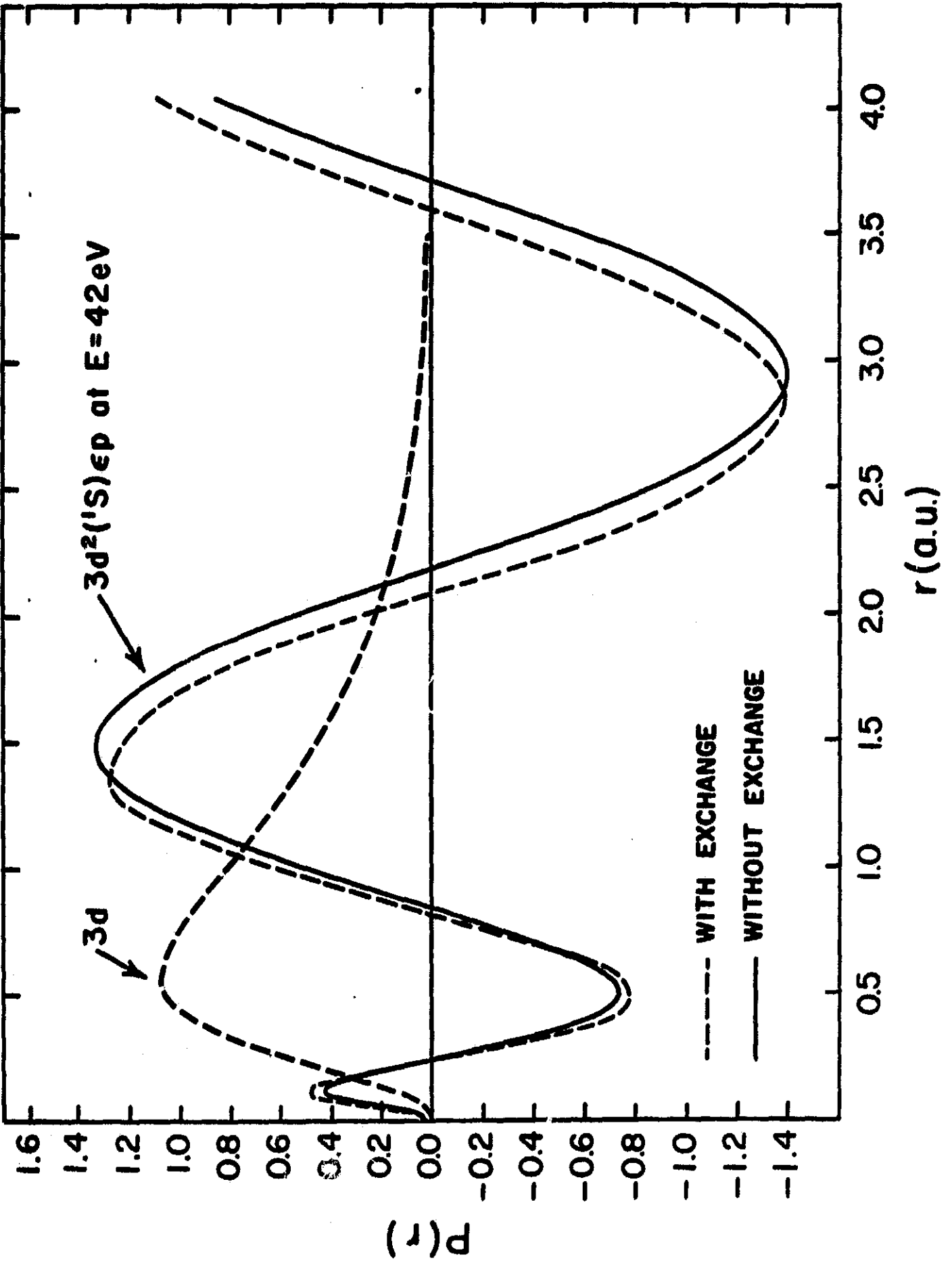
Fig. 1

Fig. 2

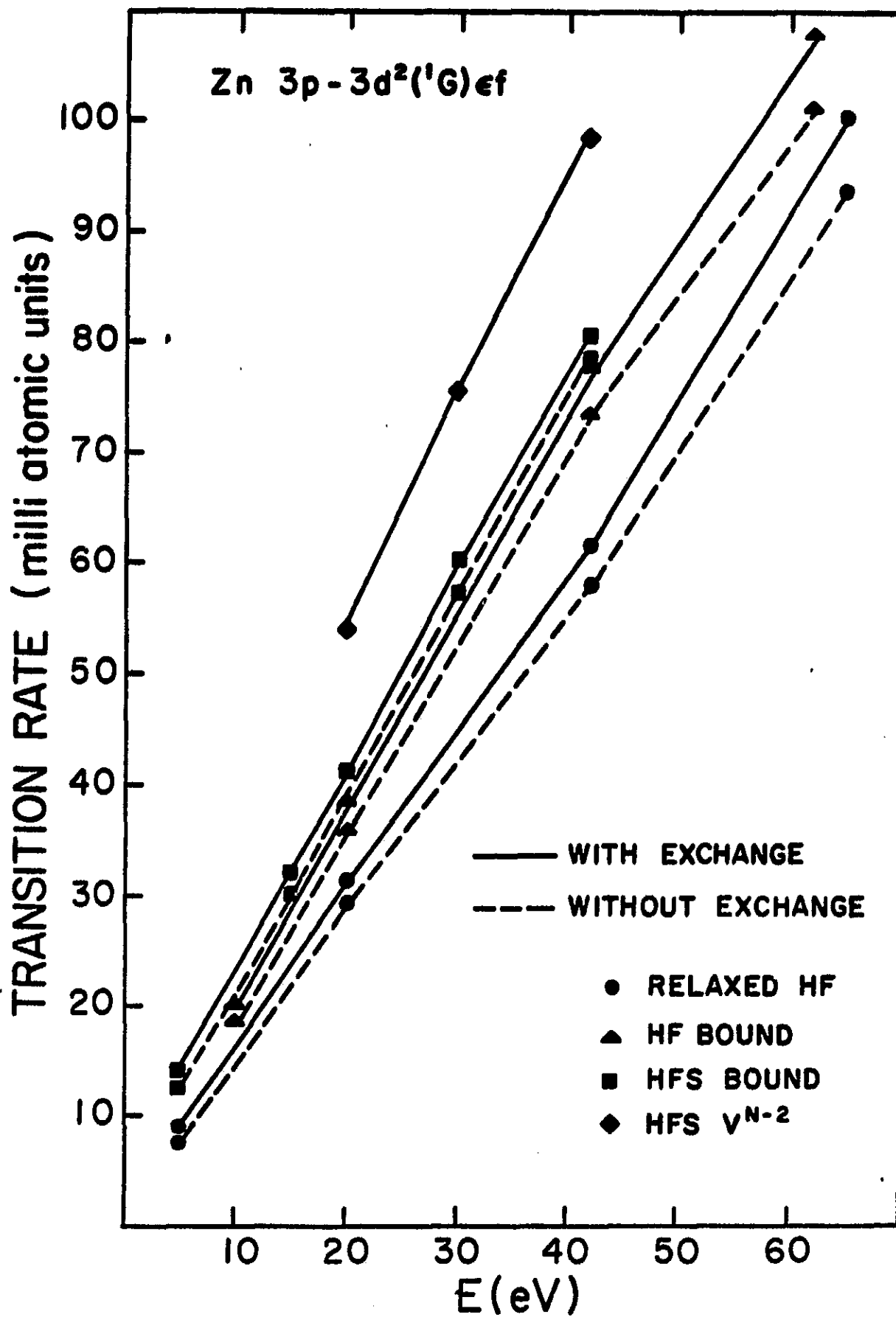$3d^2(^1S)\epsilon p$ at E=42eV

3d

—— — WITH EXCHANGE
——— WITHOUT EXCHANGE

P(r)

r(a.u.)

Fig. 3

Fig. 4